Effects of tensile strain and transverse cracks on Lamb-wave velocity in cross-ply FRP laminates

N. TOYAMA*
Research Institute of Instrumentation Frontier, National Institute of Advanced Industrial Science and Technology (AIST), Tsukuba, Japan
E-mail: toyama-n@aist.go.jp

T. OKABE
Department of Aeronautics and Space Engineering, Tohoku University, Sendai, Japan

Ultrasonic Lamb waves have significant potential for large-area, non-destructive evaluation because they can propagate a long distance. Therefore, structural health monitoring systems for composite structures using Lamb waves have become the focus of attention. Since the Lamb-wave velocity is sensitive to changes in the in-plane stiffness of the laminates, damage, such as transverse cracks and delamination, can be detected through the changes in the wave velocity [1]. However, advanced composite materials, especially CFRP, exhibit non-linear stress-strain responses [2, 3] due to the stiffening of the carbon fibers [4] and softening of the matrix resin, i.e., the in-plane stiffness depends on strain (stress). Damage detection using the Lamb-wave velocity under external loadings thus becomes more complicated. Most of the studies were concerned with detecting damage in composite laminates under strain-free conditions [1, 5, 6], and there have been few studies measuring *in-situ* the Lamb-wave velocity under loadings [7, 8].

In this study, we measured *in-situ* the Lamb-wave velocity for GFRP and CFRP laminates during tensile tests, and investigated their elastic behavior in detail. Lamb-wave detection of transverse cracks was also performed for cross-ply laminates under loadings.

The materials studied were GFRP (GE1300/TX 24235) and CFRP (T800H/3631) laminates with stacking sequences of $[0]_8$, $[90]_8$ and $[0/90_n/0]$. The average thickness of each ply and density were 0.1 mm and 1910 kg/m^3 for GFRP laminates, 0.135 mm and 1530 kg/m^3 for CFRP laminates. Tensile coupons 210 mm long and 15 mm wide were cut from a 300 × 300 mm plate, and 30-mm-long GFRP end tabs were bonded at both ends of the specimens.

The experimental set-up for Lamb-wave generation and detection during the tensile test is illustrated in Fig. 1. A pulse generator (Model 5077PR, Panametrics, Inc.) generated pulses of 500 kHz to excite a transmitting transducer (M5W, Fuji Ceramics Corporation). The pulse generator also transmitted a trigger signal to a digital oscilloscope to set the initial time. The transmitter with a diameter of 5 mm and a receiving transducer (M304A, Fuji Ceramics Corporation) with a diameter of 4 mm were glued to the surface of the specimen. The distance between the transducers was set to 100 mm. The detected signals were amplified (A1002, Fuji Ceramics Corporation) and acquired at a sampling rate of 2.5 GS/s by the digital oscilloscope, which averaged 100 samples to improve the signal-to-noise ratio.

Lamb-wave velocity under strain-free conditions was measured before the tensile test. The thickness of the specimen combined with the frequency used to generate the Lamb wave yielded a frequency-thickness product of about 0.5 MHz mm. Only the S_0 and A_0 modes propagate in this region, and the velocity of the S_0 mode is much higher than that of the A_0 mode. Therefore, the leading part of the detected wave was easily identified as the S_0 mode. The arrival time of the S_0 mode at the receiver was determined using the zero-cross point after the first positive peak, as illustrated in Fig. 2. First, in order to measure the differences in arrival times of the S_0 mode for different propagating distances, only the transmitter was glued and the receiver was placed on the specimen surface via coupling water, 20 to 120 mm from the transmitter in steps of 20 mm. Least-squares fitting from a plot of arrival time and distance was applied to obtain the velocity of the S_0 mode. The arrival time at zero distance, t_0, was obtained from the fitted line in order to calculate the *in-situ* wave velocity during the tensile test.

The tensile test was performed at room temperature with a cross-head speed of 0.5 mm/min using a universal testing machine. The tensile strain was measured with a strain gauge with a gauge length of 5 mm attached to the center surface of the specimen, and the tensile load was measured with a load cell.

In order to understand the elastic behavior of the cross-ply laminates, Young's moduli of the $[0]_8$ and $[90]_8$ specimens for both materials were evaluated as a function of strain using the wave velocity during the tensile test. The arrival times were measured in 0.05% increments of strain from zero to 1.0%, and Young's modulus was calculated as described below.

The wave velocity for strain ε can be calculated as

$$V(\varepsilon) = \frac{L(1+\varepsilon)}{t(\varepsilon) - t_0} \tag{1}$$

*Author to whom all correspondence should be addressed.

0022–2461 © 2004 Kluwer Academic Publishers

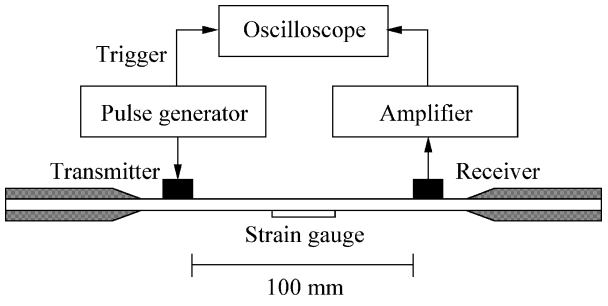

Figure 1 Experimental setup for Lamb-wave generation and detection during the tensile test.

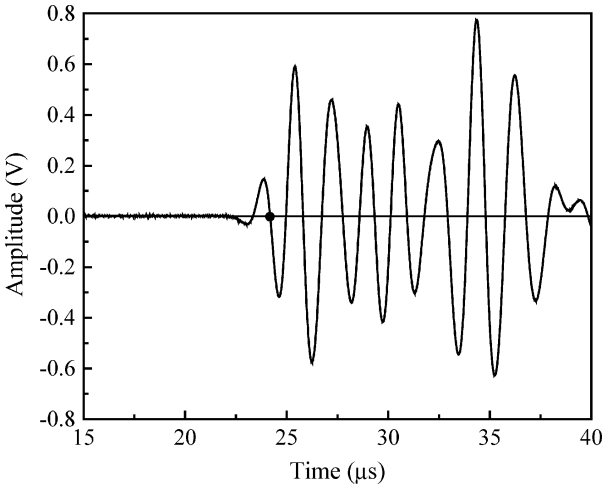

Figure 2 Leading part of the detected Lamb wave for $[0]_8$ GFRP specimen. Dot indicates the arrival time defined in this study.

where L is the initial distance between the transducers for zero strain, and $t(\varepsilon)$ is the arrival time at the receiver for strain ε.

The wave velocity in the present frequency-thickness product for the principal axis of the laminates is simply expressed as

$$V(\varepsilon) = \sqrt{\frac{E(\varepsilon)}{\rho}} \tag{2}$$

where $E(\varepsilon)$ is Young's modulus for strain ε, and ρ is the density of the laminate.

Fig. 3 presents the calculated Young's modulus as a function of strain for three $[0]_8$ specimens. Fig. 3 also depicts the tangent modulus derived from the stress-strain curve for specimen #1. The least-squares fit from a plot of strain and stress between $\varepsilon \pm 0.05\%$ was applied to obtain the tangent modulus for strain ε. Young's moduli obtained by the different methods exhibited similar values, but the scatter in the results from the stress-strain curve was larger. From these results, Young's modulus could be measured more accurately using the Lamb-wave velocity. We found that Young's modulus of the GFRP laminates was almost independent of strain, while that of the CFRP laminates increased significantly with increasing strain in this strain range. These results clearly demonstrated the different elastic behavior between glass and carbon fibers. Young's modulus during unloading was also measured.

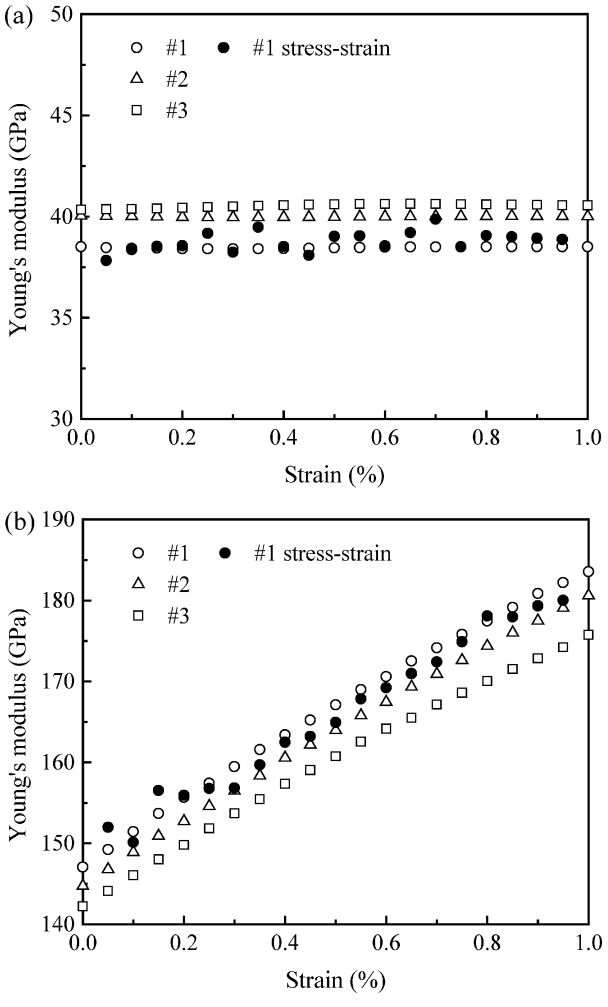

Figure 3 Young's modulus as a function of strain from Lamb-wave velocity for three $[0]_8$ specimens, (a) GFRP and (b) CFRP. Dots show the results for specimen #1 from the stress-strain curve.

Values identical to those of the loading case were obtained, and it was confirmed that the dependence of Young's modulus on strain was reversible.

The same experiments were performed on the $[90]_8$ specimens and the results are presented in Fig. 4. The failure strains for both materials were below 0.5%, so

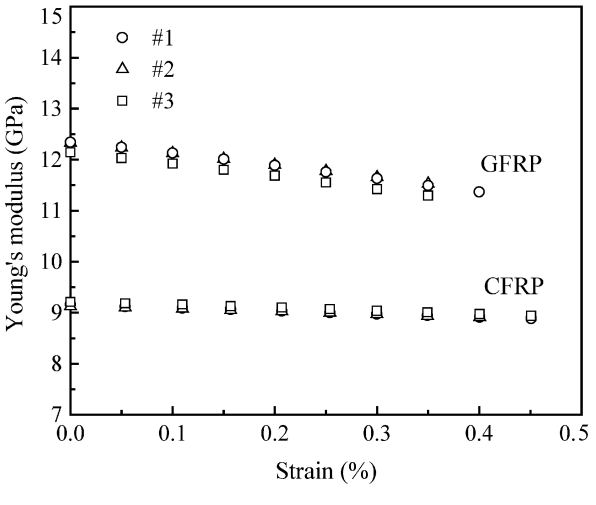

Figure 4 Young's modulus as a function of strain for three $[90]_8$ GFRP and CFRP specimens.

ranges exceeding this strain could not be investigated. Young's moduli for both materials decreased linearly with increasing strain due to the softening of the epoxy matrix.

Based on the above results, Young's moduli of the unidirectional laminates for both materials were formulized as a function of strain. The variations of longitudinal Young's modulus, E_L, of the GFRP laminates and transverse Young's modulus, E_T, of the CFRP laminates with strain were negligible. E_L of the CFRP laminates and E_T of the GFRP laminate were fitted with the averaged data using the least-squares method, and the following equations were obtained.

$$E_L(\varepsilon) \text{ for CFRP} = 144.1 + 4.134 \times 10^3 \varepsilon - 7.033 \times 10^4 \varepsilon^2 \text{ (GPa)} \quad (3)$$

$$E_T(\varepsilon) \text{ for GFRP} = 12.11 - 1.994 \times 10^2 \varepsilon \text{ (GPa)} \quad (4)$$

Fig. 5 depicts the experimental results of the normalized wave velocity as a function of strain for $[0/90_6/0]$ GFRP specimen and $[0/90_3/0]$ CFRP specimen during the tensile test. Fig. 5 also shows the crack density between the transducers. As the strain increased, the wave velocity decreased linearly for the GFRP but increased non-linearly for the CFRP below the first cracking strain. Equation 2 and the rule of mixture were applied to predict the normalized wave velocity as a function of strain for the undamaged cross-ply laminates as

$$\frac{V(\varepsilon)}{V(0)} = \sqrt{\frac{E(\varepsilon)}{E(0)}} = \sqrt{\frac{t^0 E_L(\varepsilon) + t^{90} E_T(\varepsilon)}{t^0 E_L(0) + t^{90} E_T(0)}} \quad (5)$$

where t^0 and t^{90} are the thicknesses of the 0° and 90° plies. We assumed that Equation 4 was valid beyond the failure strain of the $[90]_8$ GFRP specimens.

The predicted wave velocity is also shown as a solid line in Fig. 5. The predicted values agreed well with the experimental ones for both laminates below the first cracking strain. We confirmed that the changes in the wave velocity were due to the softening of the 90° plies for GFRP laminate and the stiffening of the 0° plies for CFRP laminate. Beyond the strain, there was a distinct discrepancy between the predicted and experimental wave velocity. Specifically, the experimental wave velocity was lower than the predicted velocity for both laminates. Cracks reduce the stiffness of the laminate, subsequently reducing the wave velocity. This stiffness reduction depends on the ratios of Young's moduli and thicknesses of the 0° plies and 90° plies. The reduction is higher as these ratios become lower. This discrepancy was thus due to the effect of the cracks. In addition to the reduced stiffness caused by the cracks, the stiffness of the 90° plies in GFRP laminates decreased further with increasing strain, but the stiffness of the 0° plies in CFRP laminates increased. Consequently, it is concluded that this characteristic behavior of the wave velocity was due to the combination of their effects. We will quantitatively analyze this in the future study.

Through our study, we could draw two important conclusions. The first one is that measuring the S_0 mode velocity is a more accurate means of evaluating the elasticity of laminates than the mechanical test. Second, the wave velocity depends on both damage and the elasticity of the laminates. Thus, damage detection using Lamb-wave velocity under loadings requires the information of the laminate stiffness as a function of strain, and the applied strain at which such measurements are performed.

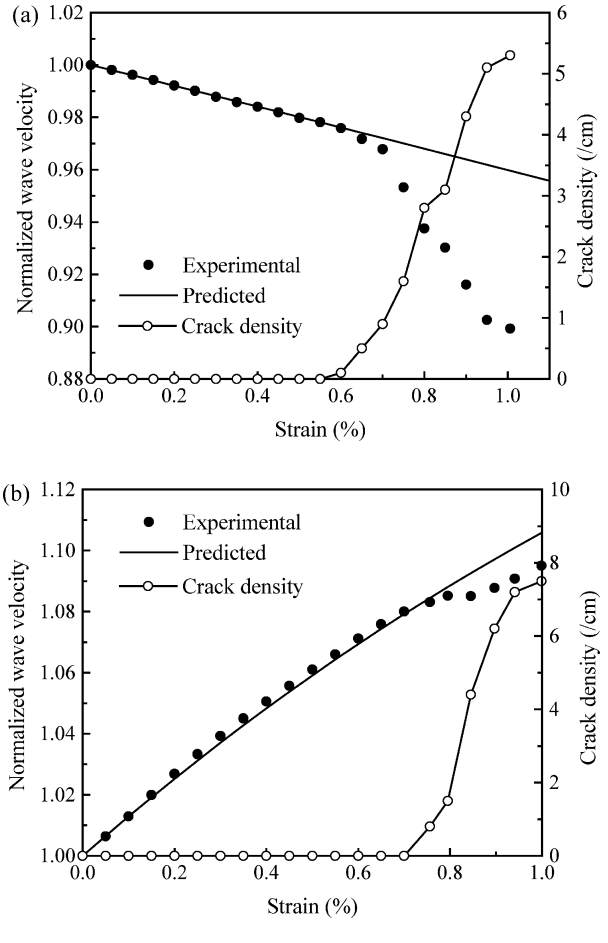

Figure 5 Normalized wave velocity and the crack density as functions of strain, (a) $[0/90_6/0]$ GFRP specimen and (b) $[0/90_3/0]$ CFRP specimen. Solid line shows the predicted wave velocity for undamaged laminate.

References

1. N. TOYAMA, J. NODA and T. OKABE, *Compos. Sci. Technol.* **63** (2003) 1473.
2. P. A. LAGACE, *AIAA J.* **23** (1985) 1583.
3. J. ABOUDI, *Compos. Sci. Technol.* **46** (1993) 51.
4. G. J. CURTIS, J. M. MILNE and W. N. REYNOLDS, *Nature* **220** (1968) 1024.
5. V. DAYAL and V. K. KINRA, *J. Acoust. Soc. Amer.* **89** (1991) 1590.
6. M. D. SEALE, B. T. SMITH and W. H. PROSSER, *ibid.* **103** (1998) 2416.
7. J.-H. SHIH, A. K. MAL and M. VEMURI, *Res. Nondestr. Eval.* **10** (1998) 147.
8. G. N. MORSCHER and A. L. GYEKENYESI, *Compos. Sci. Technol.* **62** (2002) 1171.

Received 6 April
and accepted 3 June 2004